New Ternary Alkali-Metal−Transition-Metal Hydrides Synthesized at High Pressures: Characterization and Properties

Welf Bronger* and Gudrun Auffermann

Institut für Anorganische Chemie der TH Aachen, Prof.-Pirlet-Str. 1, 52056 Aachen, Germany

Received May 13, 1998. Revised Manuscript Received June 18, 1998

Ternary metal hydrides containing both an alkali metal and a transition metal can be synthesized by the conversion of a mixture of the alkali-metal hydride and the transition metal in an atmosphere of hydrogen at temperatures between 500 and 800 K. At low hydrogen reaction pressures, only hydrides containing transition metals from subgroup eight in low oxidation states are formed. This restriction is removed at high pressures such that it is possible to prepare the following hydrides at hydrogen reaction pressures between 1500 and 5000 bar: Na_2PdH_4, $Li_5Pt_2H_9$, A_2PtH_6 (A ≙ Na, K, Rb, or Cs), A_3MnH_5 (A ≙ K, Rb, or Cs), K_3ReH_6, and A_3ReH_{10} (A ≙ K or Rb). Preliminary experiments have shown that this synthesis route also facilitates access to corresponding ternary hydrides containing the early transition metals. The crystal structures of all the hydrides mentioned were determined by a combination of X-ray and neutron-diffraction experiments on powder samples. The corresponding deuterium compounds were employed for the neutron-diffraction experiments. Additionally, susceptibility measurements were carried out on the paramagnetic compounds and interpreted, and spin structures were determined.

Contents

Introduction

In 1964, Knox, Ginsberg, and Abrahams reported the synthesis and crystal structure of the ternary metal hydride K_2ReH_9.[1] The discovery of this compound was noteworthy in a number of respects: first the unusual method of preparation that resembles alchemy, whereby potassium perrhenate was allowed to react with elemental potassium in an aqueous ethylenediamine solution, and second, its composition that finally was established only when a single-crystal structure determination using elastic neutron diffraction was carried out. The compound K_2ReH_9 was the first known alkali-metal−transition-metal hydride. It contains the $[ReH_9]^{2-}$ ion as a characteristic structural unit within which the hydrogen ligands form a coordination polyhedron around the rhenium atom consisting of a tricapped trigonal prism. In addition, the rhenium exhibits the +7 oxidation state! Even with fluorine as the ligand, an analogous compound was hitherto not known.

It was only in the 1980s that the successful syntheses and determination of the crystal structures of other ternary hydrides containing alkali metals together with transition metals proved possible. The method of synthesis involved solid-state reactions. The alkali-metal hydride AH and the transition metal M in the starting material mixture were allowed to react in an atmosphere of hydrogen in the temperature range between 500 and 800 K. Using this method, it was possible to synthesize $A_xM_yH_z$ compounds only when M is an element from the platinum-metal group. The first compound prepared in this manner in 1984 was Na_2PtH_4, which contains planar $[PtH_4]^{2-}$ structural units.[2] Over the subsequent 10 years, a whole series of ternary alkali-metal−transition-metal hydrides were discovered and structurally characterized. Table 1 contains a summary of these compounds.[3−16] Why, however, were these hydrides discovered so comparatively late? Among the various reasons, two are clearly very important: first the marked sensitivity of these substances to air and moisture that demands that their syntheses and manipulation be carried out almost exclusively in specially developed closed systems,[17] and

Table 1. Ternary Alkali-Metal−Transition-Metal Hydrides Synthesized via Solid-State Reactions at Hydrogen Pressures up to 100 bar (A ≙ K, Rb, Cs) Whose Structures are Known

metal	hydride	ref
Ru	Li_4RuH_6	9
	Na_4RuH_6	9
Rh	Li_3RhH_4	11
	Li_3RhH_6	16
	Na_3RhH_6	10
Pd	Li_2PdH_2	7
	Na_2PdH_2	6
	A_3PdH_3	8, 13
	A_2PdH_4	12, 15
	A_3PdH_5	14
Os	Li_4OsH_6	9
Ir	Li_3IrH_6	10
	Na_3IrH_6	10
Pt	A_2PtH_4	3, 4
	A_3PtH_5	5

10.1021/cm980344c CCC: $15.00
Published on Web 09/19/1998

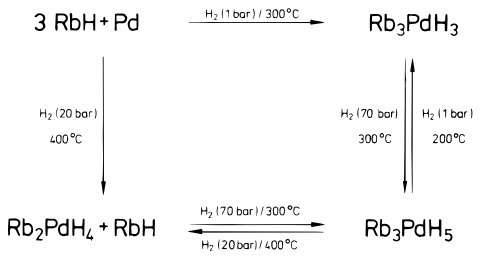

Figure 1. Experimental conditions for the syntheses of ternary rubidium palladium hydrides.

second that only in exceptional cases could single crystals of these hydrides be obtained so that determination of the crystal structures could only be performed using powder-diffraction methods. Furthermore, it was necessary, in addition to X-ray diffraction, to employ neutron diffraction on the deuterated analogues to determine the positions of the hydrogen atoms within the atomic arrangements of the metal atoms. The development of new powder diffractometers and the modern methods of analysis applied to the resulting diagrams are, consequently, closely connected with the progress in the area of the structural chemistry of the new metal−hydrogen compounds that are discussed here.

The ternary hydrides listed in Table 1 possess compositions that correspond to relatively low oxidation numbers for the transition metals. When a transition metal occurs with two different oxidation numbers in different ternary hydride compounds, one observes that an increased hydrogen pressure during the reaction stabilizes the higher oxidation number. In the field of ternary palladium hydride compounds, the system Rb/Pd/H is considered as an example in Figure 1. Whereas the hydride Rb_3PdH_3 can be prepared at normal hydrogen pressure from RbH and Pd, Rb_2PdH_4 is formed at 20 bar and Rb_3PdH_5 is only obtained when a hydrogen pressure >70 bar is used. The hydride compound formed at normal pressure contains palladium in the zero oxidation state [Pd(0)] and this is oxidized under pressure to Pd(II). As shown by the diagram in Figure 1, all three hydrides are interconvertible under suitable reaction conditions. This pressure dependence found with the formation of ternary hydrides is in accordance with the sequence of the volume increments for the hydride ion in the stated compounds.[18] One observes a decrease in the sequence RbH > Rb_3PdH_3 > Rb_2PdH_4 > Rb_3PdH_5, with the respective values, measured in cm^3/mol, of 13.0, 12.2, 11.6, and 9.2. The structures of the three ternary hydrides are reproduced in Figures 2 − 4.[13−15]In the Li/Rh/H and Li/Ir/H systems, the ternary hydrides Li_3RhH_4[11] and Li_3IrH_6[10] can be synthesized at normal hydrogen pressure from LiH and the respective transition metal. Their structures are depicted in Figures 5 and 6, respectively. In the corresponding systems involving sodium, one obtains the compounds Na_3RhH_6[10] and Na_3IrH_6.[10] These results suggested the possibility that the missing compound Li_3RhH_6 could be synthesized via the oxidation of Li_3RhH_4 with hydrogen under pressure. This suggestion indeed proved to be the case at a reaction pressure of 80 bar and revealed in a second example that high-pressure syntheses using hydrogen facilitates access to new metal hydrides.[16]

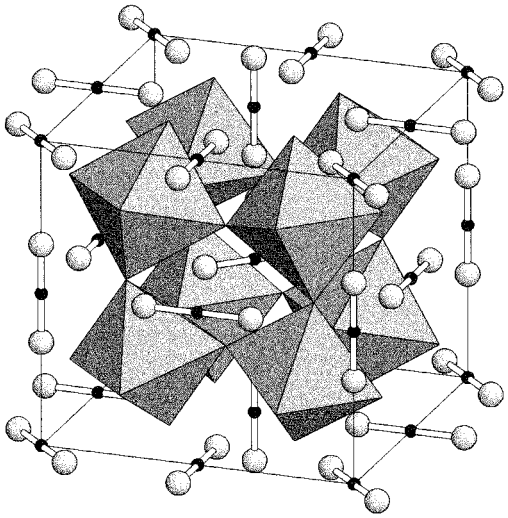

Figure 2. Atomic arrangement of the tetragonal low-temperature modification of Rb_3PdD_3, showing the vertex-sharing rubidium octahedra that are centered by hydrogen ions and the linear $[PdD_2]^{2-}$ dumb-bells.

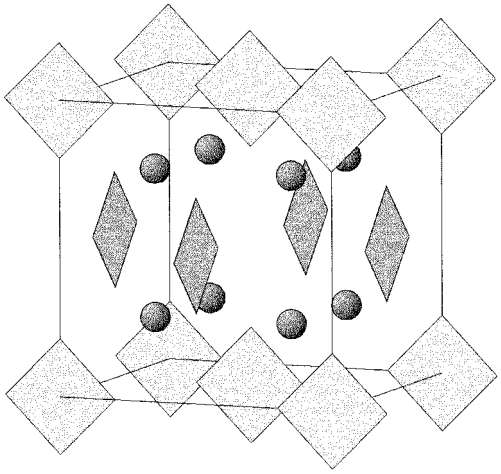

Figure 3. Crystal structure of the tetragonal low-temperature modification of Rb_2PdD_4, showing the planar $[PdD_4]^{2-}$ groups and the rubidium ions. For clarity, the structure of the low-temperature modification is represented from the same viewpoint as the K_2PtCl_6-type structure, although it may be described using a tetragonal cell that is half as large and has the following cell parameters: $a_{tetr} = a_{cub}/\sqrt{2}$ and $c_{tetr} = a_{cub}$.

New Metal Hydrides Synthesized at High Pressures: Characterization and Properties

The ternary alkali-metal−transition-metal hydrides $A_xM_yH_z$ listed in Table 1, where M is an element from the platinum-metal group, are exclusively compounds in which M occurs in relatively low oxidation states. The high oxidation states achievable in the corresponding systems containing halogens instead of hydrogen are not observed. The variation in the oxidation numbers corresponds entirely with the expectation that higher oxidation states are relatively more stable for a 5*d* element with respect to those for a 4*d* element from the same group. Consequently, one obtains under comparable conditions Na_2PdH_2[6] and Na_2PtH_4[2] or Li_3RhH_4[11] and Li_3IrH_6.[10] Additional practical experience reveals that higher oxidation states can be more easily stablized using the heavier alkali metals than with sodium or lithium.

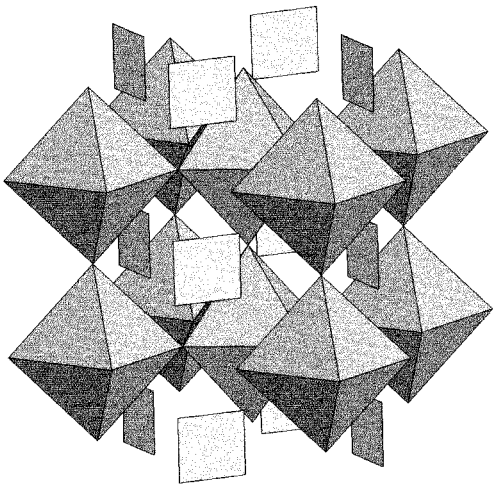

Figure 4. Rb_3PdD_5: Tetragonal framework structure of vertex-sharing rubidium octahedra centered by hydrogen ions. The space occupied by the planar $[PdD_4]^{2-}$ groups cause them to twist along the *c*-axis.

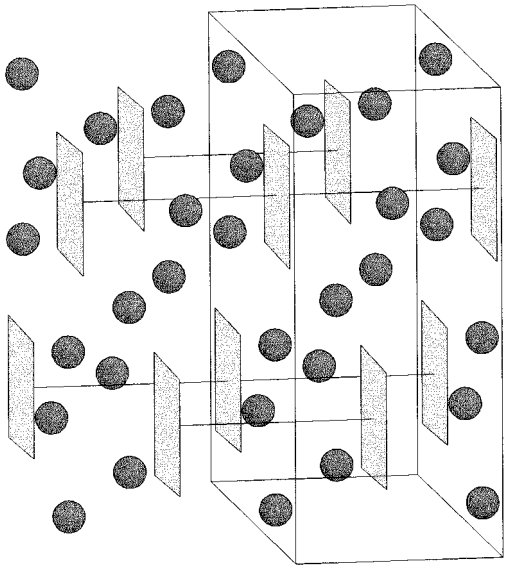

Figure 5. Atomic arrangement of Li_3RhD_4, showing the positions of the lithium atoms and the planar $[RhD_4]^{3-}$ groups.

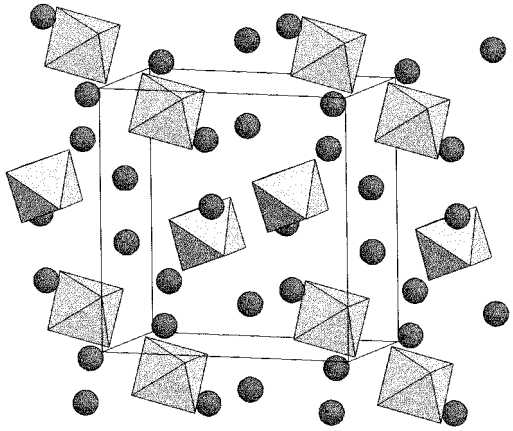

Figure 6. Orthorhombic structure of Li_3RhD_6, showing the $[RhD_6]^{3-}$ octahedra and the lithium ions.

The experiments already mentioned dealing with the preparation of hydrides using increased hydrogen pressures (for these reactions, hydrogen pressures up to 300 bar were employed) combined with the accrued knowledge that with increasing hydrogen pressure an enhanced oxidation of each transition metal investigated is possible, led to the suspicion that high-pressure syntheses may facilitate access to a field of metal−hydrogen compounds that hitherto could not be prepared. To investigate this we developed, together with our institutes workshop, autoclaves that allow continually higher hydrogen pressures to be employed.

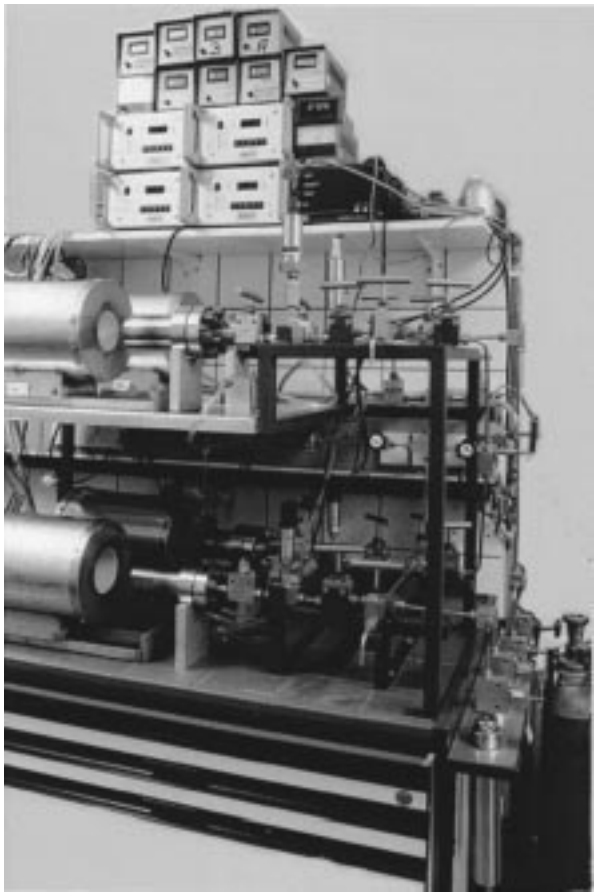

Figure 7. High-pressure equipment.

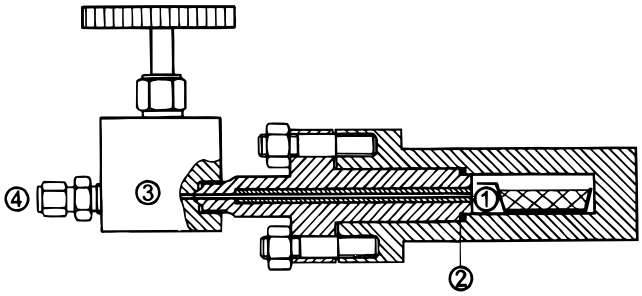

Figure 8. Schematic sketch of the high-pressure autoclave: (1) reaction boat; (2) copper gasket; (3) high-pressure valve; (4) connection for hydrogen, vacuum, and pressure gauge.

The actual high-pressure equipment used is shown in Figure 7 and a schematic diagram of an autoclave is shown in Figure 8. The high-pressure autoclaves are made from stainless steel (Coralloy 4668) and provide a reaction volume of ~14 cm^3. The autoclaves are sealed with copper gaskets. The high-pressure valves are commercially available. The high-reaction pressures are reached by the following procedure: after cooling the autoclave with liquid nitrogen, hydrogen is allowed into the autoclave from a gas bottle (maximum pressure

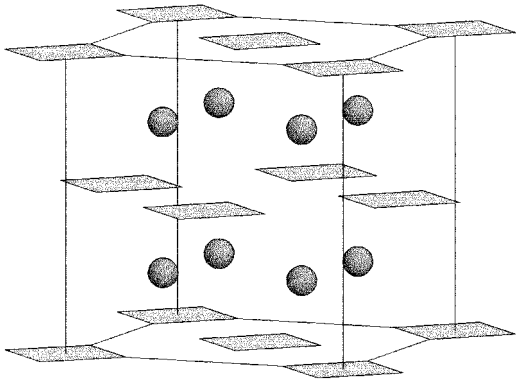

Figure 9. Crystal structure of Na_2PdD_4. The $[PdD_4]^{2-}$ squares and the sodium ions are depicted. For comparison, the structure is shown from the same viewpoint as the K_2PtCl_6-type structure, although it may be described using a tetragonal cell that is half as large and has the following cell parameters: $a_{tetr} = a_{cub}/\sqrt{2}$ and $c_{tetr} = a_{cub}$.

200 bar). This procedure allows a starting pressure at room temperature of 700 bar and a subsequent reaction pressure of ~1500 bar at 900 K to be attained. If a higher starting pressure is desired, additional hydrogen from medium-pressure storage vessels containing hydrogen at a pressure of ~800 bar and/or from high-pressure autoclaves connected in series can be transferred to the reaction autoclave. Using this technique, the required starting pressure can be adjusted by a repetition of the cooling cycle. The reaction pressure can be measured by pressure gauges specially adapted for hydrogen (maximum pressure 5860 bar). Recently, we have been successful in attaining hydrogen reaction pressures of 5500 bar at 900 K.

Using the Rb/Pd/H system as an example in Figure 1, it is evident that the Pd(0) compound Rb_3PdH_3 results from the conversion of rubidium hydride with palladium in an atmosphere of hydrogen at normal pressure. The oxidation to hydride compounds containing Pd(II) occurs in our experiments only at somewhat raised pressures of hydrogen (e.g., the formation of Rb_2PdH_4 at 20 bar[13−15]). One finds analogous circumstances exist for the systems K/Pd/H[8,12,14] and Cs/Pd/H,[14,15] but not yet for the Na/Pd/H system. In this case, the synthesis of Na_2PdH_4 is only possible at a hydrogen reaction pressure of >1800 bar and a reaction temperature of 750 K.[19] The corresponding deuteride Na_2PdD_4 has been synthesized via an analogous high-pressure experiment and its complete crystal structure was determined by neutron-diffraction experiments on powder samples. The compound Na_2PdD_4 crystallizes isotypic to Na_2PtD_4. The atomic arrangement is depicted in Figure 9. A reversible phase transition is observed for Na_2PtD_4 at 570 K. The high-temperature modification possesses an atomic arrangement that corresponds to that present in the K_2PtCl_6 type in which there is a statistical 2/3 occupation of the chlorine positions by the D atoms. For Na_2PdD_4, such a phase transition could not be observed up to 600 K. At temperatures >600 K at one bar, this compound decomposes to Na_2PdD_2, a Pd(0) compound containing linear $[D\text{-}Pd\text{-}D]^{2-}$ structural units (see Figure 10).[6]

An analogous phase transition to that observed for Na_2PtH_4 at 570 K was found for the compound K_2PtH_4 at the significantly lower temperature of 195 K. This

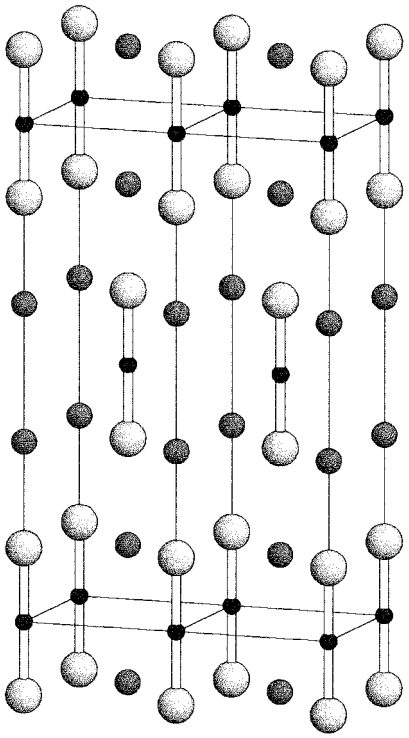

Figure 10. Crystal structure of Na_2PdD_2 showing the $[PdD_2]^{2-}$ dumb-bells and the sodium ions.

result means an atomic arrangement exists at room temperature that corresponds to that in the cubic K_2PtCl_6 type, though with a statistical occupation of the six chlorine atom positions with only four hydrogen atoms. Nuclear magnetic resonance (NMR) measurements revealed that the octahedral coordination determined for the platinum atoms is provided by fast rotational jumps by the hydrogen atoms.[20] The question still remained as to whether a further incorporation of hydrogen atoms would be possible under an increased hydrogen pressure that would lead to an oxidation of the platinum above the oxidation state two by hydrogen. Attempts to achieve this using the newly developed high-pressure autoclaves illustrated that the synthesis of K_2PtH_6, and thereby an oxidation of elemental platinum up to oxidation state +4 by hydrogen, is possible at a hydrogen reaction pressure of 1500−1800 bar and a temperature of 775 K.[21] X-ray investigations were carried out to characterize this compound, which was prepared as a colorless powder. The analysis of the diffraction diagrams showed that the platinum and potassium atoms form an arrangement analogous to that found in fluorite. The arrangement consequently also corresponds to that found in the K_2PtH_4 type. A comparison of the lattice constants of both phases revealed that the unit cell of the hydrogen-rich phase is somewhat larger.

The phase transition observed at 195 K for K_2PtH_4 does not occur for K_2PtH_6 (compare Table 2). For a complete clarification of the composition and structure of K_2PtH_6, a neutron-diffraction experiment was carried out on the correspondingly prepared deuteride analogue. The results confirmed that the platinum atoms are coordinated by a regular octahedron of six deuterium atoms and that, as a consequence, the atomic arrangement of K_2PtD_6 is isotypic to that found in K_2PtCl_6 (see Figure 11). When the occupation parameters for the

Table 2. K_2PtH_4 and K_2PtH_6: Comparison of the Lattice Constants (Å) from X-ray Diffraction Studies

	T (K)	
compound	295	9
K_2PtH_6	$a = 8.1760$ (2)	$a = 8.1116$ (2)
K_2PtH_4	$a = 8.0653$ (4)	$a = 5.622$ (1) $c = 8.122$ (2)[a]

[a] The structure of the tetragonal low-temperature modification corresponds to that of Rb_2PdH_4 (compare Figure 3).

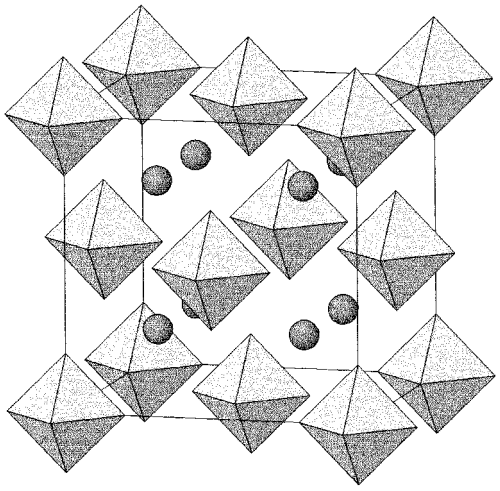

Figure 11. Atomic arrangement of K_2PtD_6. The $[PtD_6]^{2-}$ octahedra and the potassium ions are represented.

Table 3. Molar Volumes of the Hydrogen Ligands in the Hydrides A_2PtH_4 and A_2PtH_6[a]

compound	V_H^-	compound	V_H^-
Na_2PtH_4	10.0	Na_2PtH_6	7.7
K_2PtH_4	10.6	K_2PtH_6	8.2
Rb_2PtH_4	11.4	Rb_2PtH_6	8.9
Cs_2PtH_4	11.9	Cs_2PtH_6	9.1

[a] A ≙ Na, K, Rb, or Cs, in $cm^3\ mol^{-1}$; for the alkali metal ions, the following Biltz' increments ($cm^3\ mol^{-1}$) were taken: Na^+, 6.5; K^+, 16; Rb^+, 20; and Cs^+, 25.5; and for Pt^{2+}, 4 and Pt^{4+}, 0.[18,24]

deuterium positions were allowed to vary for the last refinement, a convergence was observed for K_2PtD_z when $z = 6.00 \pm 0.03$. The analogous hydrides Na_2PtH_6,[22] Rb_2PtH_6,[23] and Cs_2PtH_6[23] were also able to be prepared using the new high-pressure synthesis method. Neutron-diffraction experiments, for which the corresponding deuterides were prepared and employed, confirmed these compounds to be isotypic with K_2PtD_6. The transition from the A_2PtH_4 phase to the A_2PtH_6 phase is accompanied by a decrease in the volume increment of the hydride ion (see Table 3).[18,24]

As expected, it was found that in the area of lithium platinum hydrides, no Pt(IV) compounds could be prepared using the high-pressure synthesis method. Instead, the conversion of lithium hydride with platinum under a hydrogen pressure of 1250 bar and a temperature of 820 K resulted in a Pt(II) hydride for which the structure analysis yielded the composition $Li_5Pt_2H_9$.[25] An analysis of the neutron-diffraction diagram of the deuterated compound $Li_5Pt_2D_9$ using the Rietveld method led to a complete elucidation of the structure. The atomic arrangement as shown in Figure 12 reveals the presence of the novel anionic complex $[Pt_2D_9]^{5-}$ in which both the platinum atoms are coordinated by five deuterium ligands (Figure 13). Four of these ligands around each platinum form, within the

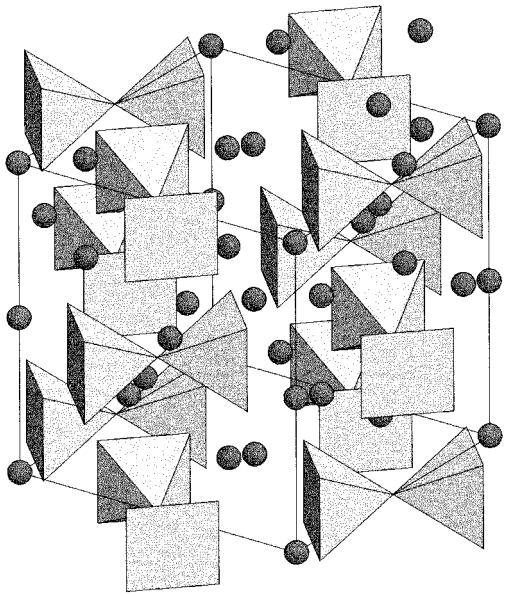

Figure 12. Crystal structure of $Li_5Pt_2D_9$. The vertex-sharing square pyramids formed by the deuterium atoms that are centered by the platinum atoms and the lithium atoms are shown.

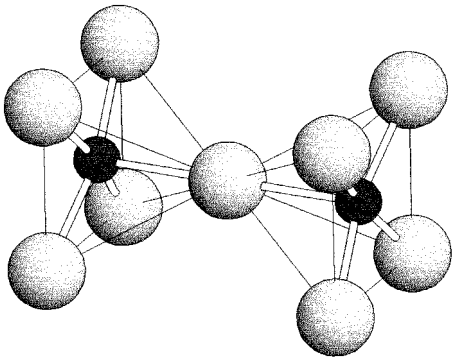

Figure 13. The $[Pt_2D_9]^{5-}$ ion.

experimental accuracy, a square planar arrangement. The platinum atom is displaced 0.196 Å from the center of the plane in the direction of the fifth deuterium atom situated at the apex of the square pyramid. The fifth deuterium atom acts as a connecting bridge to the second, identical coordination polyhedron containing the second platinum atom such that the two square pyramids are linked to one another via a common vertex. The Pt-D-Pt bridge is linear, and the two square planes of deuterium ligands per anion are arranged in an eclipsed manner with respect to each other. An analogous structure unit has, to our knowledge, not hitherto been reported. To obtain further information regarding the properties of this compound, its magnetic susceptibility was measured between 4 and 298 K. A weak, virtually temperature-independent diamagnetism was observed, which is in agreement with calculations derived from the diamagnetic increments.[26]

High-pressure syntheses to attempt the preparation of hitherto unknown alkali-metal rhodium and alkali-metal iridium hydrides are planned. In the corresponding systems involving ruthenium and osmium, ternary hydrides have been obtained under high-reaction pressures of hydrogen. The structural clarification of these compounds and thereby the determination of their exact

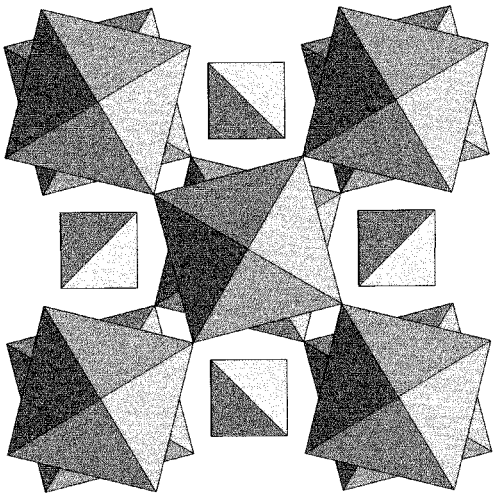

Figure 14. A_3MnD_5 (A ≙ K, Rb, Cs): Atomic arrangement showing the $[MnD_4]^{2-}$ tetrahedra and the vertex-sharing alkali-metal octahedra that are centered by hydride ions.

hydrogen content have, however, not yet been concluded.

A fundamental question posed by these experiments was whether the high-pressure synthesis method offers the possibility of synthesizing ternary alkali-metal hydrides containing *d* metals from outside subgroup eight. We can now answer this question in the affirmative. The first successes related to the synthesis of manganese compounds with the composition A_3MnH_5 where A ≙ K, Rb, or Cs.[27,28] These hydrides were prepared by the reaction of the respective alkali-metal hydride with manganese powder at 875 K under hydrogen pressures >3000 bar. The rose-colored products are extremely sensitive to moisture and air. The preparation of the deuterated analogues used in the neutron diffraction experiments proceeded similarly. A combination of X-ray and neutron-diffraction experiments on powder samples led to a complete determination of the atomic arrangements. The tetragonal I-centered structures of the three alkali-metal−manganese hydrides are isotypic and may be described in terms of framework structures of vertex-sharing alkali-metal octahedra, which are centered by hydrogen atoms. The $[MnH_4]^{2-}$ tetrahedra are incorporated within this framework. Owing to the space occupied by the tetrahedra, the alkali-metal octahedra are twisted along the *c*-axis (see Figure 14). The structural similarities between ternary hydrides and halides are again clearly obvious because this atomic arrangement is isotypic to that of $Cs_3Cl[CoCl_4]$.[29] The analogous, isotypic manganese halides and zinc hydrides are also well-known; for example, Cs_3MnCl_5,[30] Cs_3MnBr_5,[31] and A_3ZnH_5 (A ≙ K, Rb or Cs).[32,33] In addition, structural relationships with the ternary platinum-metal hydrides are plainly evident. However, contrary to the manganese hydrides, the platinum-metal hydrides contain $[MH_4]$ square planes (M ≙ Pt or Pd) or linear $[PdH_2]$ dumb-bells and not tetrahedra analogous to $[MnH_4]$ (e.g., A_3PtH_5[5] and A_3PdH_5,[14] see Figure 4; or A_3PdH_3,[8,13] see Figure 2). The high mobility of the hydrogen ligands leads to phase transitions from tetragonal to cubic atomic arrangements at higher temperatures. In the high-temperature modification, the tilting or twisting of the alkali-metal octahedra is relieved and the atomic arrangements then

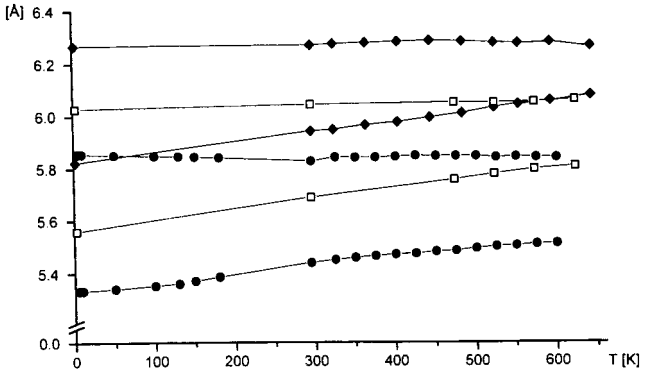

Figure 15. A_3MnH_5 and A_3MnD_5 (A ≙ (●) K; (□) Rb; or (♦) Cs): Temperature dependence of the lattice constants from X-ray and neutron-diffraction experiments. For clarity, the lattice constants are converted according to the equations: $a' = a/\sqrt{2}$ and $c' = c/2$.

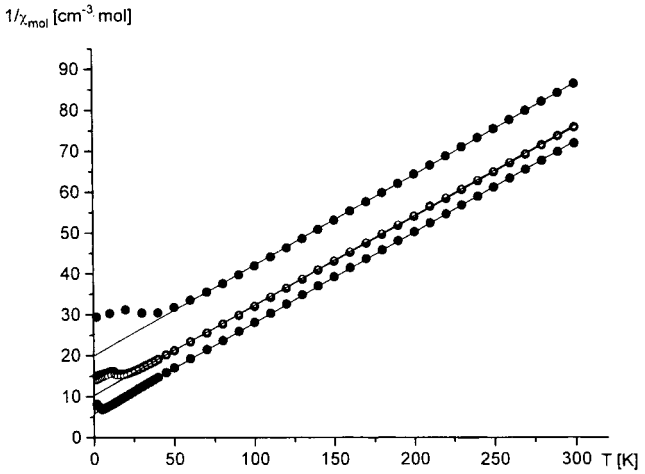

Figure 16. K_3MnH_5 (top), Rb_3MnH_5 (middle, open circles), Rb_3MnD_5 (middle, solid circles), Cs_3MnD_5 (bottom): Temperature dependence of the reciprocal molar susceptibilities ($1/\chi_{mol}$).

correspond to that of the perovskite-type structure if the transition-metal/hydrogen group is regarded as one unit with cubic symmetry. Temperature-dependent X-ray experiments on the manganese hydrides were carried out (see Figure 15) to study structural changes. A study of the variation in the lattice constants (*a*, *c*) as a function of temperature reveals that, before they can undergo a phase transition, at one bar the hydrides decompose above 575 K into the starting materials. The observed c/a values at 575 K are 1.499 for K_3MnD_5, 1.477 for Rb_3MnD_5, and 1.466 for Cs_3MnD_5 instead of the ideal value $\sqrt{2}$.

All the $A_xM_yH_z$ ternary hydrides just mentioned, where M is a transition metal of group eight, possess *d* electron configurations that result in diamagnetic behavior. The manganese compounds are the first complex transition-metal hydrides where paramagnetism is expected. In Figure 16 the reciprocal molar susceptibilities are plotted against temperature. Above the Néel temperatures the three compounds show Curie−Weiss paramagnetism. The calculated magnetic moment ($\mu = 2.828\ \sqrt{\chi_{mol}(T-\theta)}\ \mu_B$) of 6.0 (1) μ_B for all three hydrides (see Table 4) is in accordance with the expected value for an isolated $3d^5$ ion. The results from complementary neutron-diffraction experiments at low

Table 4. A_3MnD_5 (A ≙ K, Rb, Cs): Magnetic Properties from Susceptibility Measurements,[a] Field Strength,[b] and Elastic Neutron-Diffraction Experiments[c]

parameter	K_3MnD_5	Rb_3MnD_5	Cs_3MnD_5
magnetic susceptibility measurements			
weight of sample (g)	0.00221[d]	0.00319	0.00360
Néel temperature (K)	40	15	5
magnetic moment (μ_B)[e]	6.0(1)	6.0(1)[f]	6.0(1)
elastic neutron diffraction experiments			
measurement temperature (K)	8	3	2
magnetic space group	*Fm'mm*	*I*4'/*m'cm'*	I_P4'/*mcm'*
number of magnetic reflections	28	21	25
Néel-temperature (K)	28	13	4.8
magnetic moment (μ_B)[g]	4.52(5)	4.65(4)	5.07(7)
spin direction	∥*b*	∥*c*	∥*c*
⊥ *c*	antiferro	antiferro	antiferro
∥ *c*	antiferro	antiferro	ferro
R-value magnetic structure	0.044	0.057	0.055

[a] SQUID magnetometer, temperature region, 1.7−300 K. [b] 0.1−1 T. [c] Risø National Laboratory diffractometer TAS 1. [d] The magnetic susceptibility measurements were carried out on the hydrogen compound. [e] $\mu = 2\sqrt{S(S+1)}\,\mu_B$. [f] Rb_3MnH_5: weight of sample, 0.00242 g; Néel temperature, 15 K; magnetic moment, 6.0(1) μ_B. [g] $\mu = 2S\,\mu_B$.

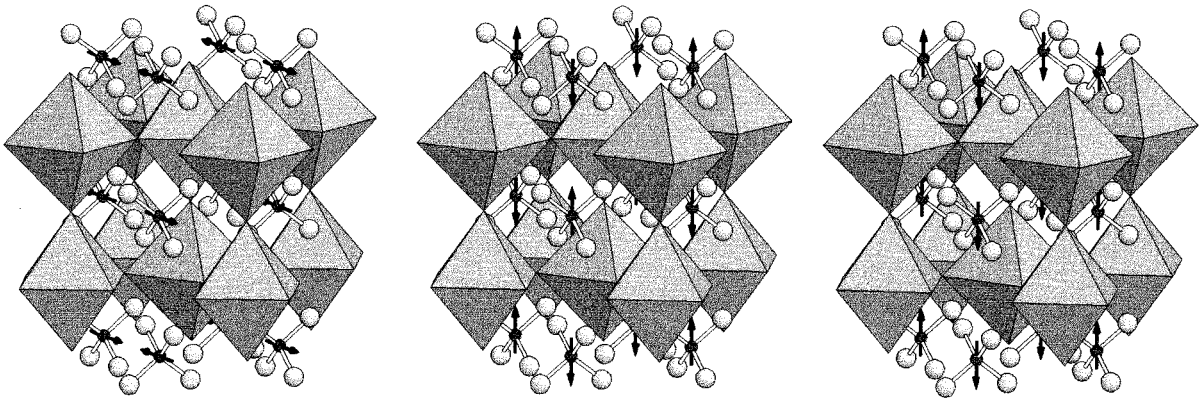

Figure 17. A_3MnD_5 (A ≙ K (left), Rb (middle), Cs (right)): Spin structures showing the spin directions, the $[MnD_4]^{2-}$ tetrahedra, and the vertex-sharing alkali-metal octahedra that are centered by deuterium ions (for clarity, the same section of the three different spin structures is always presented).

temperature confirmed the expected antiferromagnetic behavior. The profile refinements revealed different spin structures for all three compounds (see Table 4; further details are given in ref 28). The spin structures are depicted in Figure 17 (for clarity the same section of the three different spin structures is presented). Whereas the spin orientation is perpendicular to the *c*-axis for K_3MnD_5, the spin orientations for Rb_3MnD_5 and Cs_3MnD_5 are along the *c*-axis. The spins in Rb_3MnD_5 are antiferromagnetically ordered both in the (001) planes and along the *c*-axis. By contrast, ferromagnetic ordering exists in Cs_3MnD_5 along the *c*-axis, whereas antiferromagnetic ordering is again observed in the (001) planes. The three-dimensional spin ordering, occurring at comparatively high temperatures despite the relatively large Mn−Mn distances that lie in the range 5.33−6.27 Å, appears to be facilitated by super-exchange interactions via the hydrogen ligands although the interatomic D−D distances between neighboring $[MnD_4]$ tetrahedra (ranging from 3.35 to 3.73 Å) seem to be quite large. Obviously, the surprisingly high polarizablity of the hydrogen ligands promotes these interactions. No hydrides have hitherto been reported where corresponding antiferromagnetical coupling has been observed.

Because it was recognized from the synthesis of the first manganese hydrides that high-reaction pressures of hydrogen facilitate access to metal hydrides containing transition metals from outside subgroup eight, experiments were subsequently begun to investigate the preparation of corresponding rhenium hydrides.

Using a hydrogen reaction pressure of 3000−3500 bar, the first compound to be discovered from these investigations was K_3ReH_6.[34] The starting materials of potassium hydride and rhenium powder were employed in the respective molar ratio 3:1 at a reaction temperature of 850 K. The compound K_3ReH_6 is olive green in color and very sensitive toward air and moisture. X-ray investigations of powder samples and elastic neutron-diffraction experiments on the deuterated analogue led to the determination of the crystal structure. The atomic arrangement exhibits cubic symmetry and corresponds to that which exists in cryolite (see Figure 18).

Susceptibility measurements were carried out on this compound in the temperature range between 3.5 K and room temperature to determine its magnetic properties. The molar susceptibilities are shown as a function of temperature in Figure 19. A weak, almost temperature-independent paramagnetism with a χ_{mol} value of about 250×10^{-6} cm^3mol^{-1} was observed, which was corrected for diamagnetism of the constituent atoms using the sum of the ion increments.[26] The measured values reveal that the high value of the spin−orbit coupling parameter ζ evidently controls the magnetic behavior of the rhenium compound. Consequently, the electron

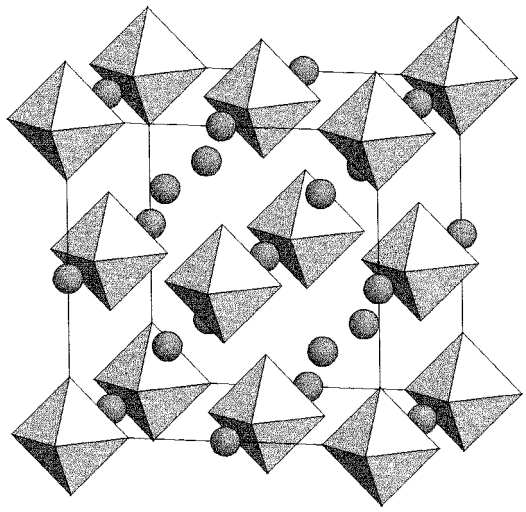

Figure 18. Atomic arrangement of K_3ReD_6. The $[ReD_6]^{3-}$ octahedra and the potassium ions are depicted.

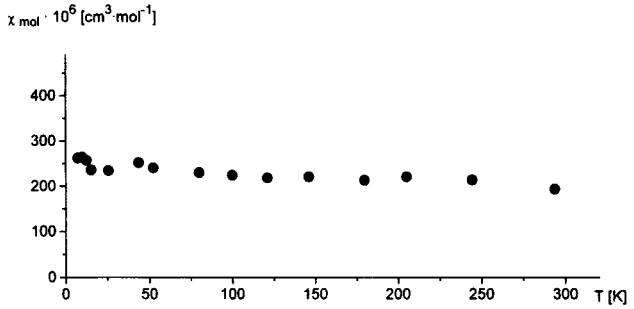

Figure 19. K_3ReD_6: Temperature dependence of the experimental molar susceptibilities (χ_{mol}).

configuration of the rhenium atoms gives rise to a ground state with $J = 0$, which allows the experimentally found weak and temperature-independent paramagnetism to be understood. This assumption was confirmed by quantum mechanical calculations[35] with which the magnetic properties of *d* element compounds may be calculated, incorporating the influence of the interelectronic interactions, the ligand field (in this case cubic), the spin−orbit interaction, and the magnetic field (Zeeman effect).

The molar susceptibility values so obtained are reproduced as a function of the ligand field parameter 10 Dq in Figure 20. A fundamental result is that, in agreement with the experiments, the susceptibility values are constant in the temperature range calculated from 1 to 300 K, which means a temperature-independent Van Vleck paramagnetism. The calculations show in detail that, as expected, the ground state is a singlet with $J = 0$. The first excited state is a triplet where $J = 1$, whose energy level depends only slightly on the ligand field strength. The $\chi_{mol} - 10$ Dq diagram reveals the increase of the second-order Zeeman coefficient with increasing ligand field strength. With regard to the ligand field strength of 10 Dq values expected here of between 12 000 and 20 000 cm^{-1}, the existence of a good numerical agreement between the measured and calculated χ_{mol} values is essentially influenced by the one electron spin−orbit coupling parameter $\zeta_{n,l}$. The value employed here for the Re^{3+} ion of 3400 cm^{-1} was estimated by means of analogy.[34] The resulting χ_{mol} values lie within the expected range.

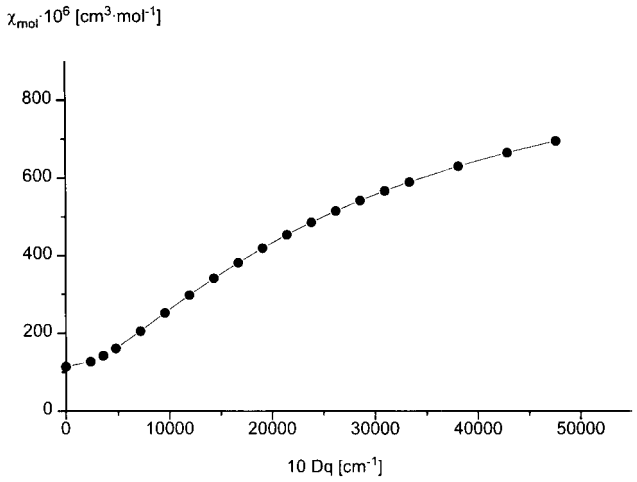

Figure 20. K_3ReD_6: Calculated molar susceptibilities (χ_{mol}) as a function of the ligand field parameters 10 Dq. Line calculated with a one-electron spin−orbit interaction parameter $\zeta_{n,l}$ of 3400 cm^{-1}; the curve does not change in the temperature range 1−300 K.

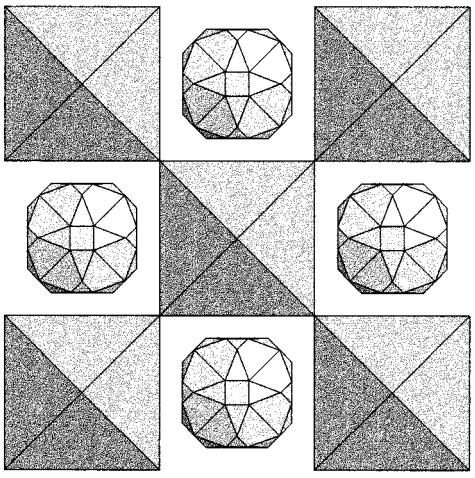

Figure 21. Crystal structure of the cubic room-temperature modification of Rb_3ReD_{10}. The vertex-shared rubidium octahedra, which have hydride ions at their centers, and the $[ReD_9]^{2-}$ groups are shown. The deuterium atoms occupy the two 24-fold atomic positions statistically with an occupation factor of 0.187(2).

By increasing the hydrogen pressure above 3500 bar, we have been able to synthesize new ternary rhenium hydrides in the temperature range between 700 and 870 K. The compounds are very sensitive toward air and moisture. Again, a combination of X-ray investigations on powder samples and neutron-diffraction experiments on the deuterated compounds has revealed the compositions K_3ReD_{10} and Rb_3ReD_{10} and allowed a complete determination of their atomic arrangements.[36] At room temperature, the primitive cubic structures of these two rhenium hydrides are isotypic and can be described in terms of vertex-sharing potassium and rubidium octahedra, respectively, which are centered by hydrogen ions. The $[ReD_9]^{2-}$ units are incorporated into these frameworks (see Figure 21). The coordination polyhedron of hydrogen atoms that surround each rhenium atom can be described crystallographically as a statistical occupation of two 24-fold positions with hydrogen with a population factor of 0.187(2). Both hydrides undergo a phase transition at low temperature. The

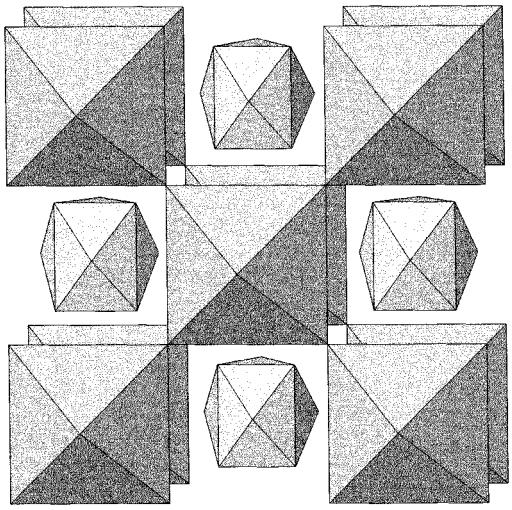

Figure 22. Crystal structure of the orthorhombic low-temperature modification of Rb_3ReD_{10} tilted along [1 1 0]. The vertex-shared rubidium octahedra, which have hydride ions at their centers, and the $[ReD_9]^{2-}$ monocapped square antiprisms are shown.

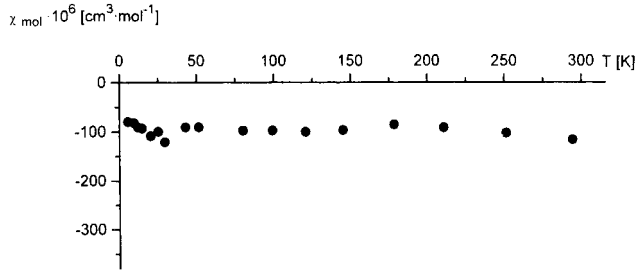

Figure 23. Rb_3ReD_{10}: Temperature dependence of the molar susceptibilities (χ_{mol}).

low-temperature modification exhibits orthorhombic symmetry. The alkali-metal octahedra are slightly distorted owing to the space required by the $[ReD_9]^{2-}$ groups, in which the deuterium atoms are now arranged in ordered positions. The hydrogen ligands form monocapped square antiprisms that can almost be considered as tricapped trigonal prisms (see Figure 22). Magnetic susceptibility measurements revealed Rb_3ReD_{10} to be diamagnetic. The observed value (see Figure 23) equals the sum of the diamagnetic increments[26] of the constituent ions ($\chi_{mol} = -97 \times 10^{-6}$ cm^3 mol^{-1}) and consequently confirms the oxidation state +7 for rhenium.

A comparison of the volume increment of hydrogen in K_3ReH_{10} with that in K_2ReH_9 already mentioned in the Introduction suggests that K_2ReH_9 is now accessible via solid-state reaction at a higher hydrogen reaction pressure than is necessary for the synthesis of K_3ReH_{10} because the volume increment of hydrogen in K_2ReH_9 is a little smaller than that in K_3ReH_{10}.

The synthesis of the compounds K_3ReH_{10} and Rb_3ReH_{10} casts a new light on the previously unique existence of the hydride K_2ReH_9. The high-pressure synthesis clearly shows that ternary hydrides of this general type exist for transition metals up to the highest oxidation states, but they are sensitive toward air and moisture to a degree that prevents their synthesis via molecular reactions in solution. K_2ReH_9 has been isolated as a product from solution only because it is not as sensitive as the other known hydrides. The fact that further such reactions were not successful in the synthesis of related hydrides explains the reclusive existence of K_2ReH_9 over the past decades.

Final Remarks

The synthesis of metal hydrides at high hydrogen reaction pressures, 5500 bar being currently achievable at temperatures of ~900 K, has opened up the way to many new compounds. Whereas only compounds of the platinum metals in low oxidation states could hitherto be obtained in the field of alkali-metal−transition-metal hydrides, the high-pressure method has now provided access to higher oxidation states and to hydrides containing transition metals from outside subgroup eight. For example, the high-pressure hydrogen synthesis method can in this way oxidize platinum up to the oxidation state +4 via the reaction $2AH + Pt + 2H_2 \rightarrow A_2PtH_6$, has made the preparation of the first manganese hydrides possible and in the field of ternary rhenium hydrides can stabilize compounds such as A_3ReH_6 and A_3ReH_{10}. Preliminary experiments have shown in addition that hydrides of the early transition metals can also be synthesized. Thus, the yellow ternary chromium hydrides $ACrH_3$, which crystallize in a slightly distorted perovskite structure,[37] have been obtained, and there are indications for the existence of alkali-metal molybdenum hydrides.[38] Generally, one can conclude that in the systems not yet investigated, the high-pressure synthesis method will facilitates access to many hitherto unknown metal hydrides.

Because high oxidation states of the transition metals can be achieved at high hydrogen pressures, as found with the synthesis of metal hydrides, one should conversely expect that intermediate states containing transition metals in lower oxidation states could result from the thermal decomposition of hydrides and one could thereby obtain access to compounds that cannot be prepared by direct means. An example of this occurs with the decomposition of the aforementioned Pt(II) compound $Li_5Pt_2H_9$, as illustrated by the following equation: $Li_5Pt_2H_9 \xrightarrow{620K} 2Li_2PtH_2 + LiH + H_2$. By this route, the first ternary platinum hydride containing platinum in the zero oxidation state could be prepared.[39] This method of synthesis is also regarded as generally suitable for the preparation of new metal hydrides.

Acknowledgment. We thank the Fonds der Chemischen Industrie, the Deutsche Forschungsgemeinschaft (DFG), and the Bundesministerium für Bildung, Wissenschaft, Forschung und Technologie (BMBF) for their generous financial support.

References

(1) Knox, K.; Ginsberg, A. P. *Inorg. Chem.* **1964**, *3*, 555. Abrahams, C.; Ginsberg, A. P.; Knox, K. *Inorg. Chem.* **1964**, *3*, 558.
(2) Bronger, W.; Müller, P.; Schmitz, D.; Spittank, H. *Z. Anorg. Allg. Chem.* **1984**, *516*, 35.
(3) Bronger, W.; Auffermann, G.; Müller, P. *Less-Common Met.* **1986**, *116*, 9.
(4) Bronger, W.; Auffermann, G.; Müller, P. *Less-Common Met.* **1988**, *142*, 243.
(5) Bronger, W.; Auffermann, G.; Müller, P. *Z. Anorg. Allg. Chem.* **1988**, *566*, 31.
(6) Noréus, D.; Törnroos, K. W.; Börje, A.; Szabø, T.; Bronger, W.; Spittank, H.; Auffermann, G.; Müller, P. *Less-Common Met.* **1988**, *139*, 233.

(7) Kadir, K.; Noréus, D. *Z. Phys. Chem. N. F.* **1989**, *163*, 231.
(8) Bronger, W.; Auffermann, G. *Less-Common Met.* **1990**, *158*, 163.
(9) Kritikos, M.; Noréus, D. *J. Solid State Chem.* **1991**, *92*, 514.
(10) Bronger, W.; Gehlen, M.; Auffermann, G. *J. Alloys Compd.* **1991**, *176*, 255.
(11) Bronger, W.; Müller, P.; Kowalczyk, J.; Auffermann, G. *J. Alloys Compd.* **1991**, *176*, 263.
(12) Kadir, K.; Kritikos, M.; Noréus, D.; Andresen, A. F. *Less-Common Met.* **1991**, *172*, 36.
(13) Bronger, W.; Auffermann, G. *J. Alloys Compd.* **1992**, *179*, 235.
(14) Bronger, W.; Auffermann, G. *J. Alloys Compd.* **1992**, *187*, 81.
(15) Bronger, W.; Auffermann, G. *J. Alloys Compd.* **1992**, *187*, 87.
(16) Bronger, W.; Gehlen, M.; Auffermann, G. *Z. Anorg. Allg. Chem.* **1994**, *620*, 1983.
(17) Bronger, W. *Angew. Chem., Int. Ed. Engl.* **1991**, *30*, 759, *Angew. Chem.* **1991**, *103*, 776.
(18) Bronger, W. *Z. Anorg. Allg. Chem.* **1996**, *622*, 9.
(19) Bronger, W.; Auffermann, G. *J. Alloys Compd.* **1995**, *228*, 119.
(20) Bronger, W. *J. Alloys Compd.* **1995**, *229*, 1.
(21) Bronger, W.; Auffermann, G. *Angew. Chem., Int. Ed. Engl.* **1994**, *33*, 1112; *Angew. Chem.* **1994**, *106*, 1144.
(22) Bronger, W.; Auffermann, G. *J. Alloys Compd.* **1995**, *219*, 45.
(23) Bronger, W.; Auffermann, G. *Z. Anorg. Allg. Chem.* **1995**, *621*, 1318.
(24) Biltz, W. *Raumchemie der festen Stoffe*; Verlag von Leopold Voss: Leipzig, 1934.
(25) Bronger, W.; à Brassard, L. *Angew. Chem., Int. Ed. Engl.* **1995**, *34*, 898; *Angew. Chem.* **1995**, *107*, 984.
(26) Weiss, A.; Witte, H. *Magnetochemie*, Verlag Chemie: Weinheim, 1973.
(27) Bronger, W.; Hasenberg, S.; Auffermann, G. *Z. Anorg. Allg. Chem.* **1996**, *622*, 1145.
(28) Bronger, W.; Hasenberg, S.; Auffermann, G. *J. Alloys Compd.* **1997**, *257*, 75.
(29) Reynolds, P. A.; Figgis, B. N.; White, A. H. *Acta Crystallogr.* **1981**, *B37*, 508.
(30) Goodyear, J.; Kennedy, D. *Acta Crystallogr.* **1976**, *B32*, 631.
(31) Seifert, H.-J.; Flohr, G. *Z. Anorg. Allg. Chem.* **1977**, *436*, 244.
(32) Bortz, M.; Yvon, K.; Fischer, P. *J. Alloys Compd.* **1994**, *216*, 43.
(33) Bortz, M.; Hewat, A.; Yvon, K. *J. Alloys Compd.* **1997**, *253*−*254*, 13.
(34) Bronger, W.; Auffermann, G.; Schilder, H. *Z. Anorg. Allg. Chem.* **1998**, *624*, 497.
(35) Schilder, H.; Lueken, H. *Computer-Programm Condon* (for calculation of magnetic characteristic parameters for d_n-systems ($n = 1-9$), with simultaneous consideration of interelectronic interactions, spin−orbit coupling, ligand field (cubic, tetragonal, hexagonal, axial), and external magnetic field), unpublished.
(36) Bronger, W.; Auffermann, G., unpublished results.
(37) Bronger, W.; Auffermann, G. *Proceedings of the VIth Conference on Solid State Chemistry*, Zürich, 1997; PA35.
(38) Bronger, W.; Auffermann, G.; unpublished results.
(39) Bronger, W.; à Brassard, L. *Z. Anorg. Allg. Chem.* **1996**, *622*, 462.

CM980344C